



An innovative geostatistical sediment trend analysis using geochemical data to highlight sediment sources and transport

Noémie Baux^{1,2} · Anne Murat^{1,2} · Emmanuel Poizot^{1,2} · Yann Méar^{1,2} · Gwendoline Gregoire^{1,2} · Sandric Lesourd³ · Jean-Claude Dauvin³

Received: 20 October 2020 / Accepted: 12 December 2021 / Published online: 28 January 2022
© The Author(s), under exclusive licence to Springer Nature Switzerland AG 2022

Abstract

To study current marine sedimentary processes and depending on the field of application, two principal approaches exist. The first is favoured by geochemists who increasingly use GIS (Geographic Information System) methodology combined with multivariate analysis (most often Principal Component Analysis and Cluster Analysis) applied to a geochemistry dataset, to analyse the spatial distribution of the chemical elements. The interpretation of results can remain complex, and the implementation of chemical elements is limited. The second performed for sedimentary studies considers three granulometric parameters (mean, sorting and skewness) that are frequently used, which are processed by Grain Size Trend Analysis (GSTA) approach, to assess the vectors of sedimentary transport. In the current study, these two distinct approaches are combined to propose a new methodology, integrating the geochemical data into a GSTA model, to assess concentration gradients. This adapted GSTA approach, named “*GSTA**”, has been tested on an existing dataset obtained from study in the eastern part of the Bay of Seine (Normandy, France) in an anthropogenic context (presence of a dumping site) to highlight the sediment dynamic processes. The results of the “classical” GSTA approach performed with granulometric parameters were compared with those from the innovative *GSTA** approach, using initially one element, Total Organic Carbon (TOC), and subsequently, three combined chemical elements, Total Organic Carbon, Calcium and Silicium (TOC, Ca and Si). The suitability of geochemical tracers in the study of coastal sedimentary dynamic and anthropogenic disturbance, according to concentration gradients is highlighted. The *GSTA** approach confirmed previous observations by Baux et al. [1] observations and enabled the identification of new short-scale processes and to determine sediment sources. It is a robust, non-subjective and informative methodology that can improve the interpretation of sediment sources and transport.

Keywords Geochemistry · Principal component analysis (PCA) · Grain Size Trend Analysis (GSTA) · Geographic Information System (GIS) · Kriging · Bay of seine · Dumping site

Highlights

- Aim: Adaptation of existing GSTA approach with geochemical parameters.
- Study of sedimentary processes, sources and transport.
- New methodology enabled the identification of new short-scale processes

✉ Gwendoline Gregoire
gwendoline.gregoire@lecnam.net

¹ Normandie univ., UNICAEN, Laboratoire des Sciences Appliquées de Cherbourg, EA 4253, 50100 Cherbourg, France

² Conservatoire National des Arts et Métiers, INTECHMER, 50100 Cherbourg, France

³ Normandie Univ, UNICAEN, UNIROUEN, CNRS, Morphodynamique Continentale et Côtière (M2C), UMR CNRS 6143, 14000 Caen, France

1 Introduction

Statistical analysis is an essential method in the study of surface processes in many disciplines: (geoscience, soil science, environmental engineering). Historically, in geochemical studies, the original approach, based on univariate statistics, have been gradually replaced since the 1980s by multivariate analysis [2, 3]. In more recent publications, PCA (Principal Component Analysis) and CA (Cluster Analysis) are the most common multivariate statistical analyses used to identify the main sources of variation in the dataset. PCA is an ordination method for establishing the correlation between samples and variables and for performing data reduction of vibrational spectra [4–7]. A growing number of studies have integrated Geographical Information System (GIS), to analyse spatial

distribution of one by one chemical element concentration. These studies associate multivariate analysis, especially to track the pollutants sources or heavy metal contamination in soil or fresh water [8–15]. Few studies incorporate subplot scores on PCA factorial axes into GIS, allowing a direct spatial analysis of the results and highlighting geochemical processes and sources [16–20, 10, 15, 21, 22].

Mc Laren [23] defined the fundamentals of Sediment Trend Analysis (STA[®]), a one-dimensional method that determines the net sediment transport pathways on the seabed. The STA[®] method is based on the comparison of statistical parameters that are mean, sorting and skewness, associated with the grain-size distributions of sediment samples. Mc Laren [23] demonstrated that relative changes in these parameters are the result of transport processes, which makes it possible to infer the directions of sediment transport. Gao and Collins [24], modified Mc Laren's initial STA[®] approach to allow a two-dimensional (2D) study renamed Grain Size Trend Analysis (GSTA). The main add-on is the definition of a characteristic distance (noted “ D_{cr} ”) representing the spatial scale on which samples are considered as neighbours. Statistical parameters are compared between a central station and samples within the characteristic distance. Poizot et al. [25] applied geostatisticals and proposed to use the semi-variogram for the statistical parameters to enable the redefinition of the characteristic distance subsequently denoted “ D_g ”. They used a regular grid of sample points obtained from the geostatistical interpolation of the initial irregular grid. A GIS software method was developed by Poizot and Méar [26] to help in the application of the GSTA methodology. The GSTA approach is used in a large number of sedimentology studies covering a wide range of different environments (sandbanks, rivers, beaches, estuaries, harbours and continental shelves; [27–32]). Yamashita [33] proposed an alternative approach, integrating eight parameters (mean and median grain size, sorting, skewness, coefficient of variation, kurtosis, mud and gravel contents). These authors used the PCA multivariate analysis to determine the weighting factor of each of the granulometric parameters. Trend vectors are calculated from the scores attributed to the principal components (named approach “P-GSTA”). The GSTA approach is mainly applied to a granulometric dataset. Nevertheless, in a few cases, geochemical studies have also been carried out using the GSTA approach [18, 22]. In these latter studies, the geochemistry dataset is processed separately from GSTA model. These authors used the results of sediment trends vectors direction to interpret the presence and transport of the chemical elements.

Many geochemistry and sedimentary methods exist to study the sedimentary processes, but few studies have combined several methods. However, identifying the origins of sedimentary material and the dynamic processes is still challenging, with respect to the increasing of anthropogenic coastal disturbances. Recently, Baux et al. [1] used granulometric

and geochemical datasets and perform multivariate analyses, combining PCA with GIS methods to study the dynamic processes and impact of the presence of a harbour dumping site (Octeville dumping site) in the eastern part of the Bay of Seine (France). In this study, the dynamic processes are interpreted according to chemical elements variability maps and gradients were hand-drawn on the map. In common with many workers who have studied sources and sediment transport [34–37, 11, 14, 15, 21], Baux et al. [1] were subjected to a number of constraints in representation of their results (developed in the discussion).

The objective of the present study is to develop an innovative methodology, to assess the sedimentary dynamic processes and sources using geochemical elements. It is proposed to adapt the GSTA approach to incorporate a chemical dataset to: (1) map chemical trends gradient vectors through a robust statistical approach limiting the amount of subjective interpretation; (2) better highlight informative results; (3) simplify the interpretation of these results. Based on Baux et al. [1] which describe the dynamics of sediment transport at a sea dumping site, the same dataset is used here to assess this new approach, and to compare it with classical methods. Various treatments were applied: (1) mapping the spatial distribution of the interpolated concentrations of each studied chemical element; (2) presentation the spatial distribution of the PCA analyses results; (3) performing the “classical” GSTA approach based on the three grain-size parameters; (4) proposal of an “innovative” integration of the chemical parameters into the GSTA model.

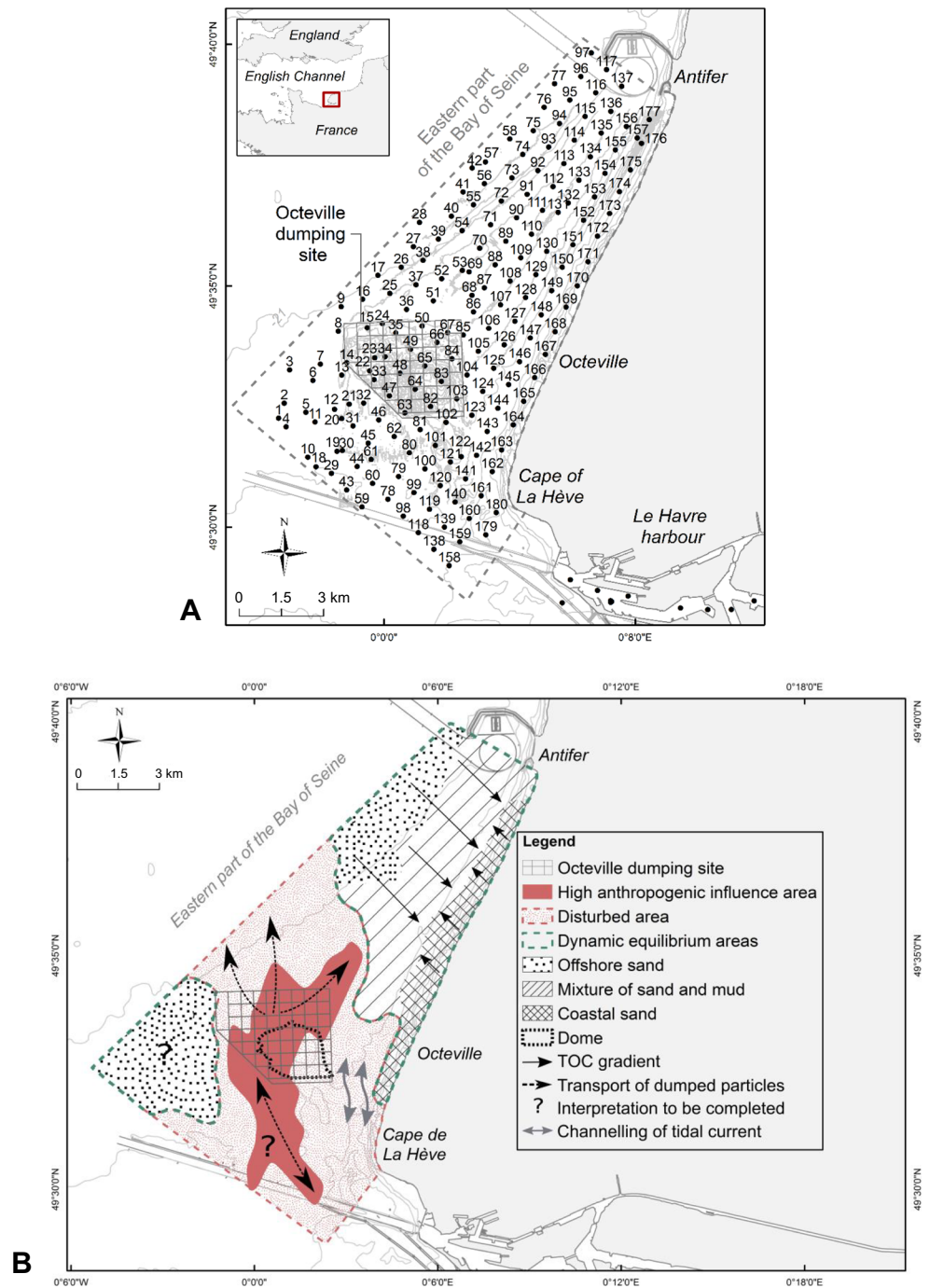
2 Study area

The study area is located in the eastern part of the Bay of Seine in the north western France (English Channel), between Le Havre harbour and Antifer harbour (Fig. 1A). Detailed characteristics are accessible in Baux et al. [1] and summarized here.

The maximum water depth is 30 m and the tidal range in spring water reaches 7.5 m [38–40]. Tidal currents trend mainly towards the northeast (NE) during flood tide and towards the southwest (SW) during ebb tides. At the beginning of the flood tide, the Antifer current runs along the coastline and turns towards the Seine Estuary. At the end of the flood tide, the current is reversed (“Verhale current”) and flows towards the NE, but still following the coastline. At the ebb, a new reversal of the water flow occurs, with the current directed towards the SW [40–42].

The Seine estuary is a major source of fine particles in the eastern part of the Bay of Seine and also in the harbour basins of Le Havre. The average annual discharge from the Seine river is estimated as $435 \text{ m}^3 \cdot \text{s}^{-1}$ rising to $534 \text{ m}^3 \cdot \text{s}^{-1}$ over the last decade [43]. The average supply of fine particles is

Fig. 1 **A:** Study area showing location of sampling points; **B:** Map summarizing the results from the study including the separation of areas in dynamic equilibrium from those that have been disturbed (from Baux et al. [1])



estimated as $6 \times 10^5 \text{ t.y}^{-1}$ (ranging from $1.3 \times 10^5 \text{ t.y}^{-1}$ to $1.7 \times 10^6 \text{ t.y}^{-1}$; [43]). Along the coast, the turbidity plume from the Seine estuary develops to a width of over one kilometre, even in the absence of waves [44]. The deposited mud is unconsolidated and thus easily resuspended by tidal currents [43].

The seafloor of the study area is mainly covered by muddy sands, with sandy muds, sands and pebbles along the coast [43]. In the region between Cap de La Hève and the Cap d’Antifer, previous studies have highlighted, a coastal fringe

where the fine fraction ($<63 \mu\text{m}$) makes up between 10% to 25% of the sediment, and with spatial and temporal fluctuations in the mud content [38, 39, 45, 46].

A lot of human activities are present in and around this area (fisheries, passenger transport, marine aggregate extraction, harbour activities, etc.), including the Havre harbour dumping site (named Octeville dumping site) used since 1947 and located 8 km from the harbour entrance. Since 2006, the Le Havre harbour dredged $2.5 \text{ to } 3 \times 10^6 \text{ m}^3 \text{ y}^{-1}$ in average, mainly composed of mud (on average, 80% $<63 \mu\text{m}$ fraction

for 2009–2014; [47]) The SE sector of the dumping site corresponds to a historical deposition area associated with a shoal (rising 5 m with respect to minimum sea level in Le Havre harbour = “Cote Marine du Havre”, CMH) and coarse sediments. Dumped sediments are deposited to the N, NW, and SW of the dumping site, following a system of “boxes”, in which the sediment is distributed in a thin layer of between 0.1 to 0.6 m per box per year.

Geochemical study conducted by Baux et al. [1] provide additional information on the fine particles dynamic. With a combination of multivariate statistical analyses (PCA - Principal Components Analysis and CA - Cluster Analysis) and GIS methods, these authors highlighted several dynamic processes taking place in the study site and identified four distinct areas (Fig. 1):

(1) In the NE area, two increasing TOC gradients have been identified which are perpendicular to the isobaths. The first TOC gradient observed increases from offshore (25 m depth) to around 15 m isobath and the second TOC gradient, from the coastline (5 m depth) to the same isobath. The convergence at around 15 m water depth corresponds to an area with Organic Matter (OM) accumulation, due to the lowest energy level. The coastal zone is a shallow water area with high-energy swell and weak tidal currents, in opposition to the deeper offshore area, where the situation is reversed, with tidal currents more energetic than the swell. The two observed gradients display a sedimentary dynamic equilibrium state. (2) In the SW part of the study area, a similar pattern is observed on a smaller scale, with TOC gradient from the offshore towards the dumping site.

(3) On the dumping site, sediments are rich-in TOC, rubidium (Rb), organic bromine (BrOrg), sulphides (S) and lead (Pb), due to the constant dumping of anoxic harbour fine sediment. Around the dumping site, the particles transported remain finer over time and are also enriched in OM in contrast to the natural sediment that stays in a dynamic equilibrium state. The TOC gradients converge towards the dumping site. The structured pattern of TOC gradients allows to delimit the area disturbed by the dumped dredge spoil.

(4) In the SE part of the study area, between the dumping site and the coast, the presence of the historical dumping site (forming a dome 5 m depth) close to the coast, impacts the trajectory and intensity of tidal currents, leading to the accumulation of organic-poor sands.

3 Methodology

3.1 Sampling strategy and laboratory analyses

A total of 179 stations (set on a regular grid, with spacing of 500 m between stations) was sampled in January and February 2016 using a 0.04 m² Shipek grab aboard the GPMH ship “Le

Marais”, between the Cap de la Hève and the Antifer harbour (Fig. 1A). Laser diffraction particle-size analysis (Beckman Coulter LS 13320) was carried out on the fine superficial sediment and elemental contents were determined by X-ray fluorescence (xSORT) and by infrared spectrometry (LECO CS 744) to assess Total Organic Carbon (TOC) content. The sampling strategy and laboratory analyses are described in detail in Baux et al. [1].

3.2 Data processing

3.2.1 Multivariate statistical analysis methods

The results of multidimensional analyses PCA and CA performed by Baux et al. [1] are used in this study. The purpose of PCA is to find synthetic representations of large numerical datasets generally by using 2D plots. If the initial spaces of statistical units and variables representation have too many dimensions, it is impossible to visualize the data cloud. We therefore look for spaces with few dimensions best fitting the data cloud. Principal Components Analysis chooses the first PCA axis as that line goes through the maximum variation in the data.

The objectives of this study were (1) to gradually reduce the number of geochemical parameters and, (2) to select the best markers for discriminating samples from each other. Seven discriminant constituents are recognized in Baux et al. [1]: Si (silicon), S (sulphide), As (arsenic), BrOrg (organic bromine), Rb (rubidium), Pb (lead) and TOC.

3.2.2 Selected chemical elements

The TOC and BrOrg are both markers of OM contents and Rb is a marker of clay mineral [48]. These elements are present in a large part of the study site, as a result of the harbour activities (dredging) and also by the flow of the River Seine. Baux et al. [1] define these elements as dynamic tracers, highlighting the natural dynamic in the NE part of the study site. Si marks the coarse detrital fraction observed on both side of the OM enrichment area [1]. Here, the As, Pb and S are excluded due to their limited spatial extend. Within the studied area, Ca marks (1) actual marine biologic sources, coarse sediments and (2) fine carbonates transported in the Bay of Seine by the river from the Paris basin. Ca is thus included in this work to identified sediment sources.

3.2.3 Geostatistical analyses

Geochemical data were previously standardized to a distribution with an average of 0 and a standard deviation equal to 1 (Eq. 1).

$$x = \frac{X - \mu}{\sigma} \tag{1}$$

where μ is the mean; σ the standard deviation; X the raw value and x the standardized value.

As the geochemical elements were measured at particular spatial locations, their interpolation allows to better highlight the spatial distribution and identify the sources.

The geostatistical data enabled the analysis and modelling of spatial variations of processes which evolved across the study area. Of the various methods present for analysing geostatistical data, the semi-variogram [49] is one of the most commonly used (Eq. 2).

$$\gamma(h) = \frac{1}{2} E_{|y-x|=h} [(Z(x) - Z(y))^2] \tag{2}$$

where $\gamma()$ is the half average squared differences between pairs of data values, i.e. $Z(x)$ and $Z(y)$, separated by a lag distance h , which is the distance separating two experimental points.

When a complete semi-variogram analysis is conducted on a regionalized variable, it enables the definition, if it exists, of a spatial model of variation of the studied parameter. This model can be used, for example for interpolation, used to complete the set of spatial knowledge of a variable at unsampled locations.

The semi-variogram calculations were performed using R.3.5.2 software (“Rgeostats” package; [50]) on standardized data. A variographic model is performed for each chemical element, PCA results and grain size parameters [51]. Ordinary kriging is the most widely used geostatistical interpolator and is based on a model of stochastic spatial variation [52]. Extra data points have been interpolated from the original dataset and the geostatistical model and a regular grid coverage 500 m were created, according to the recommendations of Poizot et al. [25, 51].

3.2.4 Grain Size Trend Analysis (GSTA): The classical approach

The Grain Size Trend Analysis (GSTA) approach was developed to highlight sediment transport processes based on the spatial trend variations in grain size parameters [23, 24, 53, 54]. These sediment transport pathways were modelled using three major grain size statistical parameters: mean size, sorting and skewness. The compilation of these three parameters produces eight possible combinations (Table 1). Two of these scenarios have a high probability of occurring between two sediment samples and are the most common cases employed: The first is “FB-” where the grain size distribution become finer, better sorted and more negatively skewed in the direction of sediment transport and the second is “CB+” where the grain size distribution become coarser, better sorted and positively skewed in the direction of sediment transport [23].

Table 1 List of possible cases for Grain Size Trend Analysis based on three-grain size parameters

Sedimentological trends	Definition
FB+	$\mu_A < \mu_B, \sigma_A > \sigma_B, SK_A > SK_B$
FB-	$\mu_A < \mu_B, \sigma_A > \sigma_B, SK_A < SK_B$
FP+	$\mu_A < \mu_B, \sigma_A < \sigma_B, SK_A > SK_B$
FP-	$\mu_A < \mu_B, \sigma_A < \sigma_B, SK_A < SK_B$
CB+	$\mu_A > \mu_B, \sigma_A > \sigma_B, SK_A > SK_B$
CB-	$\mu_A > \mu_B, \sigma_A > \sigma_B, SK_A < SK_B$
CP+	$\mu_A > \mu_B, \sigma_A < \sigma_B, SK_A > SK_B$
CP-	$\mu_A > \mu_B, \sigma_A < \sigma_B, SK_A < SK_B$

μ : the mean grain size; σ : sorting (standard deviation); SK: skewness. The suffixes A and B represent two samples. F: Finer (mean), C: Coarser (mean); B: Better sorting; P: Poorer sorting; +: positively skewness; -: negatively skewness

Poizot et al. [25, 42, 51] and Poizot and Méar [55] have proposed some modifications to consider the model uncertainties and established optimal method recommendations. These authors recommend the use of a regular interpolated grid and the calculation of the geostatistical distance (D_g) through a semi-variogram analysis [25]. Some methodology have been developed to performed GSTA, in particular the “GiSedTrend” plugin fitted into GIS software by Poizot and Méar [26], which allows the calculation of sediment trend vectors having direct access to environmental data. This plugin was merged into QGis (until the 2.18 version). The significance of any results was tested with a non-parametric test integrated in the plugin. This calculation was performed after the definition of the trend vectors at each sample location and took into account the spatial dimension of the analysed data [55]. The size of the trend vectors is proportional to the level of confidence associated with the specified direction.

Furthermore, the GSTA is conducted, here, with the three sedimentary parameters (mean, sorting and skewness) of each sample from the study site ([1]) from regular grid and a variographic settings model. Vectors are interpreted as the more likely direction of transport of sediment from a location. The length of vectors is in relation with the level of confidence of the transport. Transport direction is an interpretation of the trend vectors field.

3.2.5 Geochemical Sediment Trend Analysis (GSTA*): A novel approach

To obtain gradients of the concentration of selected chemical elements, an approach based on GSTA was applied to geochemical data. The GiSedTrend plugin was used, replacing the statistical grain-size parameters with chemical data, from a variographic model and a regular grid. To use this plugin, the mean, sorting and skewness data were replaced by chemical parameters (Tables 1 and 2). With the adaptation of the GSTA

Table 2 Defined cases for GSTA* approach, correspondence with the gradients of chemical elements concentration names and the four cases in the GiSedTrend plugin

	Concentration trend			Corresponding GSTA group
	TOC	Ca	Si	
HHH	+	+	+	FP+
HHL	+	+	–	FP-
HLH	+	–	+	FB+
HLL	+	–	–	FB-

+: gradient from least to most concentrated; –: gradient from most to least concentrated. H: Higher concentration; L: Lower concentration; F: Finer (mean); B: Better sorting; P: Poorer sorting; +: positively skewness; –: negatively skewness

method, a new set of scenarios was defined. With three parameters, eight trend cases can potentially be defined, according to the concentration studied trends (higher “H” or lower “L”) for each element.

On the studied area, to characterize the mobility of the dredged deposits, the focus is on the fine particles for which the TOC is the best marker. Thus, in a first step, to validate the GSTA* model, one chemical element, the TOC, is firstly integrated in the plugin. In the second step, three chemical elements, TOC, Ca and Si, were introduced to perform the GSTA* approach.

Four cases were selected according to the direction of gradients for each chemical parameter investigated. H (higher) trend correspond to an increase in concentration from point A to point B. L (lower) trend correspond to a decrease in concentration from point A to point B. To highlight the mobility of the fine particles and fine sediment-sink areas, the trend of increasing TOC (H) was chosen. The concentration of other chemical elements increases (H) or decreases (L) depending on the case: HLL, HLH, HHL and HHH (Table 2). Correspondences between geochemical concentration trends and sedimentological trends is also presented in Table 2. As an example, HLH case represents an increase of TOC content and a decrease for both Ca and Si concentration.

4 Results and discussion

4.1 Interpolated maps: Mapping one by one each chemical element

The interpolation of the concentration of each chemical element is the easiest way to study the spatial distribution of sedimentary geochemical data and to identify the sources. In the present study, the interpolated values of standardized chemical element concentrations were calculated with respect

to the semi-variographic model results and the spatial distribution of the concentration chemical elements were obtained by ordinary kriging interpolation on a regular grid (interval of 500 m).

Calcium, which is a marker of sediment sources and biological material, was distributed homogeneously over the study site (Fig. 2). A very high concentration was observed on and around the historical dumping site (the SE part of the dumping site), due to the accumulation of old dumped sediments [1].

The distribution of Si (Fig. 2), a marker of the coarse detritic fraction, can be interpreted as the localisation of coarse sediments. Medium and coarse sands (>250 µm) are mainly distributed at north-eastern and north-western regions of the study site, along a coastal fringe and offshore. Another area is observed at south-western part of study site, composed of clean sand. Coarse sand is also present on the historical dumping site.

Concentrations of TOC, BrOrg and Rb are mainly associated with the finest sediment (<63 µm), around and on the actual dumping site and also along the coastal line. Baux et al. [1] highlighted a grain size sorting and an accumulation of OM at around 15 m depth (Fig. 1B), according to the convergence of swell and tidal currents (creating a region of low energy). Rb is highly concentrated in the north-eastern coastal area, where coarse glauconite-rich sand has been identified (Fig. 2).

The interpolated maps of the TOC, BrOrg and Rb (Fig. 2) present very similar characteristics patterns and redundant information. In fact, visual comparison of spatial distribution maps is a commonly used method [18, 8–15, 22]. The interpolation map allows representing the parameters or the chemical elements one at a time (Fig. 2). Nevertheless, this requires the assessor to “manually” associate the parameters or/and the chemical elements to each other, making the interpretation difficult and sometimes subjective. Moreover, the number of maps produced and interpreted can be sometimes very considerable. This is the case in the work carried out by both Duman et al. and Li et al. [18, 22], who studied marine sediment sources with an approach similar to that reported here. They mapped, respectively, the spatial distribution of 10 and 21 chemical parameters. It was therefore impossible to optimize the interpretation in this way. The large number of maps may have led to a considerable reduction in the quality of the comparison of the various parameters and their geographical variability. To deal with this shortcoming, it is necessary to combine several parameters within the same statistical analysis giving rise to a single map.

4.2 Multi-element mapping

The multivariate statistical analysis enables the combination of several chemical elements to obtain one synthetic

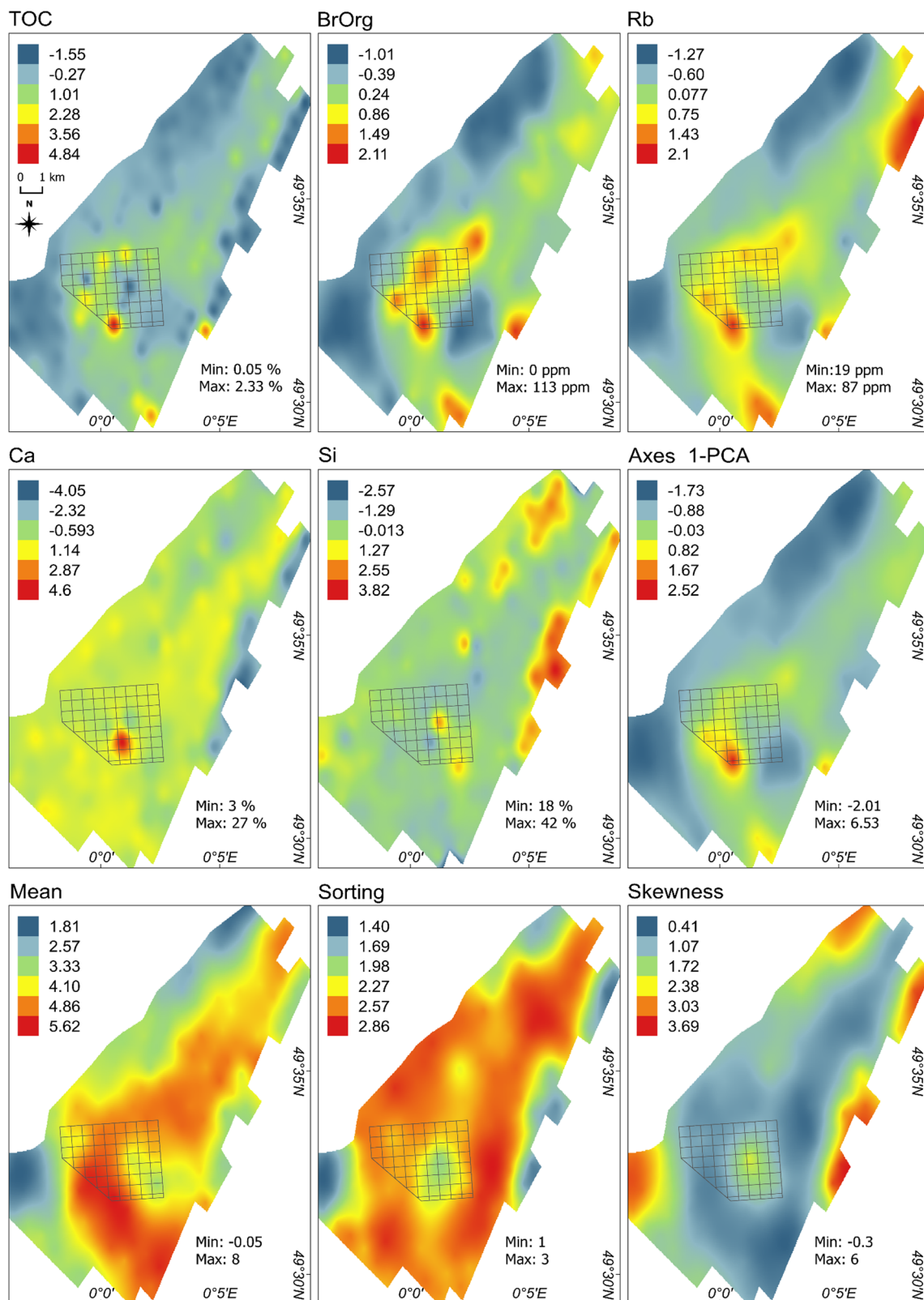


Fig. 2 Spatial distribution of standardized chemical elements concentration (TOC, BrOrg, Rb, Ca and Si), the axis 1 of PCA previously performed by Baux et al. [1] and grain-size parameters (mean, sorting and skewness). Maps were obtained by ordinary kriging interpolation from a regular grid (interval of 500 m). Values are displayed

by a range of colours from deep blue (lowest) to red (highest). The minimum and maximum of the raw values are given at the bottom right of each respective map. The marked grid and grey square correspond to the current and historic dumping sites respectively

interpretative map. Numerous multivariate statistical methods exist (PCA, CA, PMF, AFC, NNMF). In a review, Hou et al. [14] compare 29 soil heavy metal studies among which 19 studies used the PCA method (66%) and 13 CA (45%), which makes CA, the second most used method of multivariate analysis and the PCA, the most commonly used multivariate ordination method. PCA enables the identification of sources (for example, in the case of a heavy metal pollution; [14, 21]) or the determination of the limit of an impact caused by anthropogenic activities [56, 1] and can be used to infer potential sources from geochemical properties of sediment [33]. Two studies, close to our concerns, focused on the geochemical sources of the sediment [18, 22]. This was carried out using alternative methods, PMF (Positive Matrix Factorisation) and FA (Factor Analysis) based on Q- and R-modes. Usually these methods are respectively used to assess atmospheric pollutions or human behaviour [57–62] and are rarely used to study sedimentary processes.

In the present study, the Kriging interpolation was applied to visualize the spatial distribution patterns for scores of the axis 1 of the PCA, using the same method as for chemical elements (Fig. 2). This interpolated map enables the combination of several elements, especially TOC, BrOrg, Sulphide and Pb, which are concentrated in the finest sediment in and around the dumping site. The same spatial conclusions were obtained from the PCA results. However, in comparison with the single element map, this approach provides more information.

The interpretation of this type of map needs supplementary information to understand the conditions of transport and deposition of the sedimentary particles. In several studies, Duman et al. [18], Baux et al. [1] and Li et al. [22] studies, need the precise knowledge of the physical parameters present on their study areas to interpret the chemical results, but the data on tidal currents or energy levels were not always available. To assess the transport of sediment, these authors can use a complementary method, the GSTA approach.

4.3 Classical GSTA

The spatial distributions of the three granulometric parameters are interpolated using the same methodology as for the chemical parameters: results are presented on Fig. 2. The interpolated map of the mean particle size shows an accumulation of finer particles on the dumping site, locally on the coastline near the dumping site and in a region running from the dumping site towards the north-eastern the southern parts of the study site. This pattern is also observed on the sorting interpolated map, with high sorting values (> 2.7) found in the area running from the southern to north-eastern part of the study site yet excluded the historical dumping site. High values for this parameter are also observed along the southern coastal

fringe and in offshore, around the dumping site. Mapping results for the skewness of the particle size distribution show the opposite trend: high values for skewness (> 2.9) are mainly distributed along the coastal areas, those in the north-eastern sector, in the area running from offshore to the north-western sector and in the south-western part of the study site.

For the study site, the findings provided by the spatial distribution of the three granulometric parameters does not provide additional information to the multi-element mapping. It is the same observation as made by Duman et al. [18] and Li et al. [22], who map the spatial distribution of the percentages of silt, sand and clay. In contrast, the GSTA approach, used with the three grain size parameters, allows the statistical illustration of sediment trend vectors and the identification of the sediment transport pathway [23, 63, 64, 51].

Following Poizot and Méar [55] a semi-variographic analysis is realized to assess the structuration of data. Semi-variograms for the mean, sorting and skewness (Fig. 3) show similar characteristics and reveal a low spatial dependency and relatively high accuracy. The y intercept of the fitted curves relatively deviates from the origin (the nugget effect), indicating that a measurement error is present with a statistical noise which reflects a poor structuration of fine-scale processes. Only the large-scale processes can be interpreted with a relative high confidence level.

Grain-size trend vectors were calculated by using the “GiSedTrend” plugin for QGIS software [55]. The two most common cases presented in the literature are tested [53, 54, 64]: the first case is FB- (sediments were better sorted, finer and negatively skewed in the direction of transport) and the second case is CB+ (sediments become better sorted, coarser and positively skewed; Fig. 4).

Once interpolated on a regular grid, the three granulometric parameters are used to compute sediment trends. In the CB+ case (Fig. 4B) trend vectors reflect the evolution from finer to coarser sediments. Vectors are directed mainly from muddy areas towards offshore fine and medium sand areas and towards coastal areas. Some transport vectors also illustrate movement towards the historical dumping site. These areas exhibit coarse sediments (in a mixture of fine and medium sand in offshore area and in gravels on the historical dumping site) in opposition with actual dumping site and the stripe running from dumping site to the north-eastern part of the study site, which exhibit a fine sediment rich in organic matter [1]. On a fine stripe offshore of the study area, CB+ vectors are oriented from the southern to the northwestern part of the study site, parallel to the coast, assuming that the sediment is not expelled outside the studied area. The boundary between the disturbed and undisturbed area (as described by Baux et al. [1]) in the NE sector, is well defined, except that near the coast which is a very complex area. On the disturbed area defined by these authors (Fig. 1), the interpretation of the set of grain size trend vectors is also complex, largely because the coarse

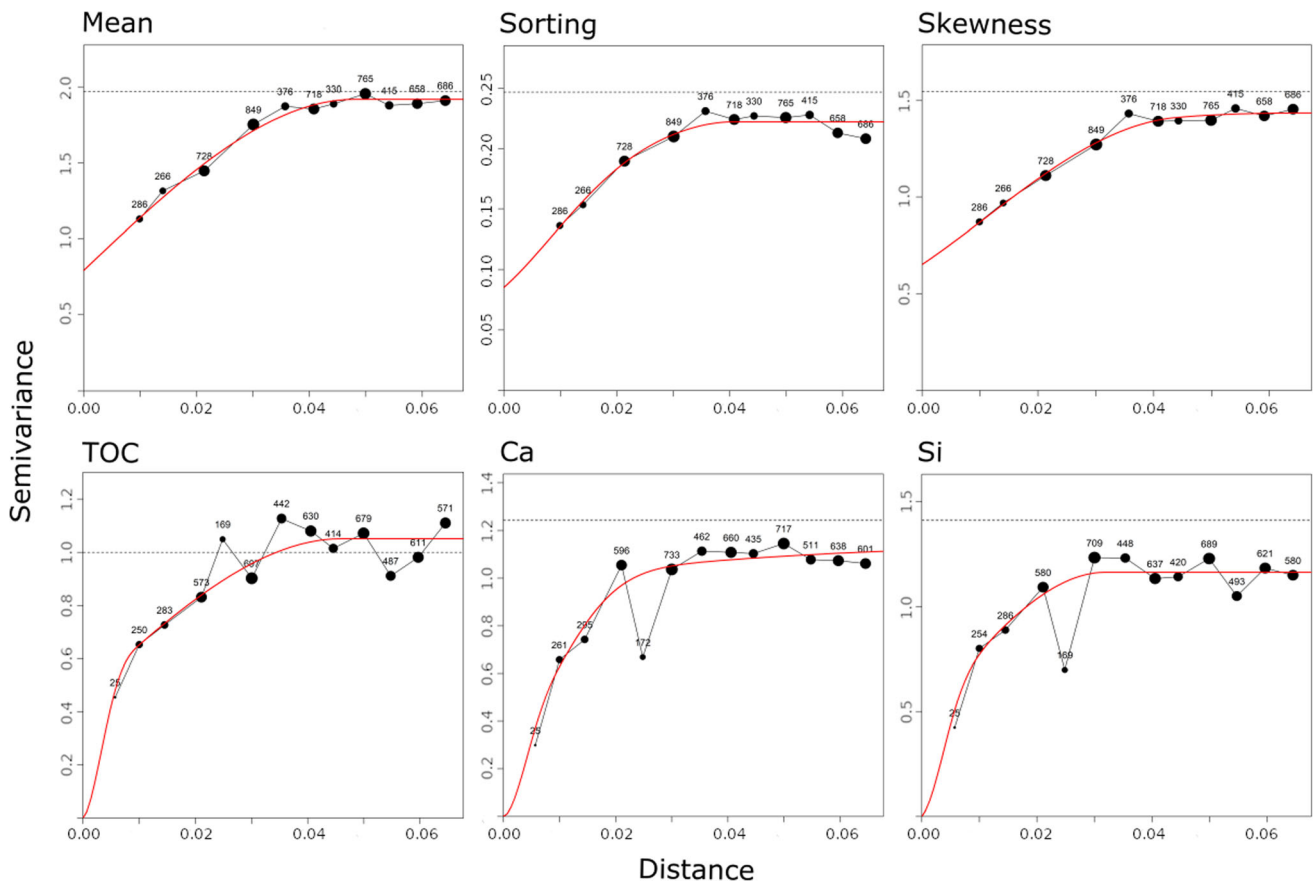


Fig. 3 Experimental semi-variograms (black dotted line) and fitted variogram models (red line) for the statistical parameters of the grain size and for three of the chemical elements chosen for the GSTA approach (TOC, Ca and Si). The model that produces the smallest residual error was chosen independently for each parameter: a spherical model for the Mean, Sorting, TOC and Si parameters; a combined

spherical and cubic model for the Skewness; a combined gaussian, spherical and cubic model for the Ca parameter. Values for TOC, Ca and Si are standardized to set the average of the distribution to 0. Distances are in decimal degree. The size of the black dots in the experimental semi-variograms is proportional to the number of pairs use to compute the semi-variance value

sand is locally distributed in this area (on historical dumping site and on a region of high-energy) and progressively enriched with fine particles.

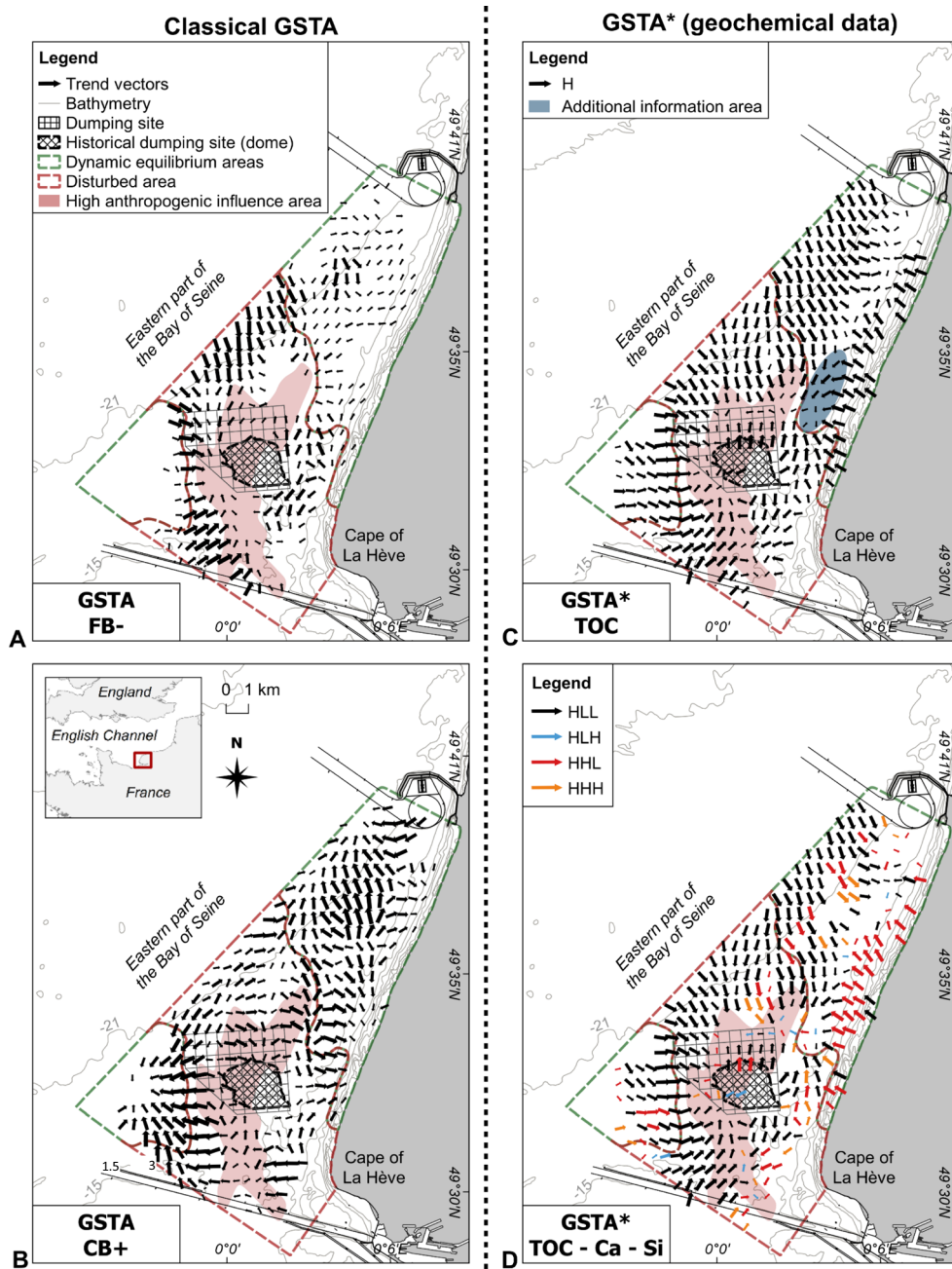
The coarser sediments are generally less mobile, any movement observed only in a high energy level environment. In opposition, the transport of fine sediment is continuous because the fine particles are more readily suspended, with rapid changes. A continuous supply of fine particles from natural sources (the Seine estuary) and from anthropogenic sources (the dumped sediments from harbour basins), contributed to the high instability of the fine sediment fraction. There is a great deal of interest in the study of the dynamics of fine sediments. The FB- case, which reflects the evolution process from coarser to finer sediments, is more appropriate here.

In the FB- case (Fig. 4A), the trend vectors are mainly directed towards the dumping site. Several areas can be clearly distinguished. A sediment refinement is discernible in the following areas: (1) from offshore towards the dumping site, (2) from the southern part of the study area and navigation channel towards the dumping site, and (3), from the coastal area

moving along of southern and northern parts of dumping site. This last example of dispersion is due to the reduced depth of the seabed, brought about by the historical dumping site (up to 5 m CMH) and also because of its proximity to the coast, which creates a narrowing zone where the water currents are increased (channelling of tidal currents) and fine particles are thus expelled [1]. These three patterns of trend vectors highlight fine sediment accumulation areas, almost exclusively on and around the dumping site. Compared to interpretation given by Baux et al. [1], the disturbed area has been correctly identified by these trend vectors. Nevertheless, the area of dynamic equilibrium is not clearly highlighted with the GSTA method. The trend vectors are absent in the SW region and minor (i.e., with a low confidence) in the NE sector.

There is still some problems relating to the GSTA method itself which are discussed in the literature: trend types, definition of characteristic distance, smoothing of vectors, and tests to determine significance of results. [26, 51, 64, 65]. The GSTA approach does however enable the identification of the direction of sediment transport. On the study site, the most

Fig. 4 Grain size trend vectors (A and B) and geochemical trend vectors (C and D) with delimitation of disturbed and dynamic equilibrium areas from Baux et al., ([1]; *c.f.* legend on A). **A:** classical GSTA case FB-performed on grain-size parameters; **B:** classical GSTA case CB+ performed on grain-size parameters; **C:** innovative GSTA* approach performed on TOC concentration (H case); **D:** innovative GSTA* approach performed on the concentrations of TOC, Ca and Si (see Table 2 for further description of the cases). H: Higher concentration; L: Lower concentration



conventionally used CB+ case is not appropriate and the FB-case better highlights the dynamic and the dispersion of fine sediments on the anthropogenic area (on and around the dumping site); however, the natural sedimentary processes (at the NE) are not clearly identified. Moreover, the semi-variographic analyses indicate that measurement error exists in a shorter distance. This is explained by the presence of many samples with a plurimodal distribution on the study site, causing errors when estimating the grain size parameters, especially the mean size. Yamashita et al. [33] highlighted the same problem in their study of a hydrodynamical environment with mixed transport processes, when using height

granulometric parameters (mean and median grain size, sorting, coefficient of variance, skewness, kurtosis, mud and gravel log-ratios) performed into a PCA. These authors concluded that the P-GSTA approach allows to reconstruct sediment transport patterns under mixed sediment transport processes in comparison with classical GSTA approach. Nevertheless, in a first way, it is regrettable that the authors didn't use the protocol proposed by Poizot and Méar [26] but instead compared their P-GSTA to the established GSTA method which is known to be difficult when applied to a mixed sediment environment. In a second way, their semi-variographic studies and models (Fig. 6 in Yamashita et al.

[33]), reveals a high uncertainty at short distance, in particular, for the parameters of skewness and kurtosis, for which the model's choice is questionable. The relative success of the P-GSTA approach is likely to be relevant only on studied sites such as those used by Yamashita et al. [33].

In the new results reported here, the results of semi-variographic study were not satisfactory in a shorter distance it was thus decided to focus on the geochemical parameters to describe the sedimentary processes and to propose the GSTA* approach (*c.f.* section 4.4).

Moreover, both the GSTA and GSTA* approaches require a precise preliminary semi-variographic study to establish the degree of confidence to be placed in the results at the finest scale and define the scale of interpretation. This scale can vary widely according to the site studied and involve different objectives. In this present study site, the area covers 160 km² compared to 3000 km² for the work of Duman et al. [18] and 38,400 km² for that of Li et al. [22]. The density of samples is also very different, with ~1.12 samples per km² in this present study, contrasted against ~0.03 samples per km² in Duman et al. [18] and Li et al. [22]. The differences in the geographical scales and in the sampling density do not allow the study the sedimentary processes at the same scale [66]. For each scale of study, the sampling density corresponds an interpretation scale. In the present study, the relatively high density of sampling enables a higher resolution in the interpretation of the sedimentation processes occurring in relation to the dumped. This is in contrast to the work reported by Duman et al. [18] and also and Li et al. [22], both of whom studied sediment sources at a larger scale.

4.4 GSTA* (GSTA adapted to geochemical study)

4.4.1 Method validation with TOC

The new methodology proposed under the name GSTA* was firstly tested using the TOC concentration which enabled the identification of the gradients and mobility of fine particles (Fig. 4C).

The semi-variogram for the TOC values (Fig. 3) reveals a good spatial dependency. The *y* intercept of the fitted curves goes through the origin (i.e., the nugget effect is zero for the model), indicating both that measurement error are insignificant and that the processes studied at a fine scale can be interpreted with confidence. The fine-scale TOC values structuration is better than the granulometric semi-variograms. The *D_g* chosen for the GSTA* model based on TOC concentration was 0.046 dd (~ 500 m). The corresponding semi-variogram study exhibited a high degree of reliability meaning that this method was promising for the study site.

To applied GSTA* approach on TOC content in the “GiSedTrend” plugin, the values corresponded initially to the mean are replaced by the interpolated TOC data and a

trend is defined in the direction of increasing value of TOC concentration (H). The trend vectors directions (Fig. 4C) are in accordance with those reported by Baux et al. ([1]; Fig. 1B) and provide a more precise information base for interpretation. In the northern part of the study site, two opposite TOC gradients are observed: (1) from the coast to the offshore area and (2) from the offshore area to the coast. The TOC accumulation between these two regions is clearly identified by a change of direction and a reduction in the size of the TOC vectors. The undisturbed area at the NE is clearly marked out. In the southern part of the study site, trend vectors are directed towards the dumping site, where fine particles, rich in OM content, were accumulated. On the dumping site itself, TOC gradients are directed towards the northern part, where harbour sediments are mainly dumped. An area where TOC accumulates was observed in the south-eastern part of the study site, spatially under the dumping site, with the TOC vectors oriented towards the south. Finally, the GSTA* model provides supplementary information, close to the NE part of the dumping site (shown on Fig. 4 C), which are comparable with the interpretations of Baux et al. [1]. Many of the gradients are oriented towards the dumping site, indicating an influence of the dredged sediment on the OM accumulation at the NE part of the study site. This information really exists in the dataset and the high sampling density enabled its validation. However, previously, on the base of considering the raw data only, and despite the high sampling density, this information was not detected.

The developed GSTA* model precisely defines several areas with different sedimentary OM dynamic. Geochemical parameters can reveal the dynamic processes associated with sediments. In the context of the dredge deposit studied, the chemical concentration trend can be interpreted as the direction of transport from the sediment source area to sediment sinks area, areas where is finally deposited (sediment sinks area).

Interpretations assessed by experts are under influence of their scientific background and that entices them towards already known ideas. The developed GSTA* model is a non-subjective, informative and interpretation aid useful methodology. Provided trends result from calculations with a geostatistical analysis as prerequisite leading to an improvement of the robustness of the interpretation.

4.4.2 GSTA*: A full three elements application

Following on from the promising results from applying the GSTA* model to a TOC dataset, a second GSTA* implementation was conducted using three distinct chemical parameters: TOC, Ca and Si, replacing respectively the “mean”, “sorting” and “skewness” values. These three chemical elements were tracers of different sources and may supply various additional

information. It is interesting to challenge these three chemical parameters in a GSTA* analysis.

Tracing the changes in Si and Ca concentration enables the identification of the origin of sediment, with the Si as marker of detritic fraction and coarse sediments and the Ca as marker of fine carbonates originating from Seine estuary and biological coarse material. The semi-variograms for Ca and Si were very similar and reveal a good spatial dependency (Fig. 3). The y intercept of the fitted curves goes through the origin (i.e.; the nugget effect is null), indicating again that measurement errors are insignificant and a great structuration at the fine-scale distance. The Dg value chosen to this GSTA* model was 0.046 (~ 500 m), corresponding to the highest values of the three calculated Dg (as discussed by Poizot et al. [25]).

The case HLL (black vectors) is logically dominant across the study site (229 vectors on of the 263 vectors, Table. 2). This scenario reflects a TOC concentration gradient running from low to high concentrations, in opposition to the concentration gradients for Ca and Si which can be interpreted as a gradient of refinement. TOC is mainly present in fine sediment, whereas Ca and Si are associated with coarser particles. In this HLL case, the granulometric factor is dominant. Trend vectors of HLL case are directed from offshore (both north and south) towards the dumping site and from the coast towards the offshore, reflecting the presence of a large quantity of fine particles on study site and along a stripe extending from the dumping site to the north-eastern part of the study area.

The simultaneous presence of high concentrations of Si and TOC along with a low concentration of Ca (blue vectors in Fig. 4, case HLH) is incompatible in this study site, where TOC is present on the finest sediment and Si in the coarser sediments. Consequently, the case HLH is poorly represented (only 13 small vectors) and can be considered negligible.

The cases HHH and HHL (distinguished by orange and red vectors respectively in Fig. 4) are observed predominantly along a coastal fringe and at the northern part of study site, on both sides of the area where OM accumulates and to the south of dumping site. The case HHL (74 red vectors) are less apparent than the case HLL but it still provides some useful information:

- (1) The littoral coarse sand is mainly composed of a high Si content and a low Ca and TOC concentration (Fig. 2). The interpolated Ca concentrations (Fig. 2) highlight the presence of this element in the fine sediment. The Si-rich littoral sands become finer to the offshore area, with an increase in concentration of Ca and TOC. This case can be interpreted as the gradient of refinement and reflects the transition areas between terrigenous littoral sand and the sediments that are rich-in OM.
- (2) The offshore siliceous sands become Ca and TOC-rich to coastal area. This HHL case corresponds to a gradient from siliceous to carbonate sands enabling some

interpretation of the sources of particles (continental or marine).

Finally, considering the case HHH; this indicates that TOC, Ca and Si concentrations change when moving in the same direction. This case is observed in the highly hydrodynamic areas; that is, between the dumping site and the coast and also at the North in the offshore region of the study site. This is the most complex case (represented by 26 orange vectors in Fig. 4) and can be explained by several distinct causes in different locations:

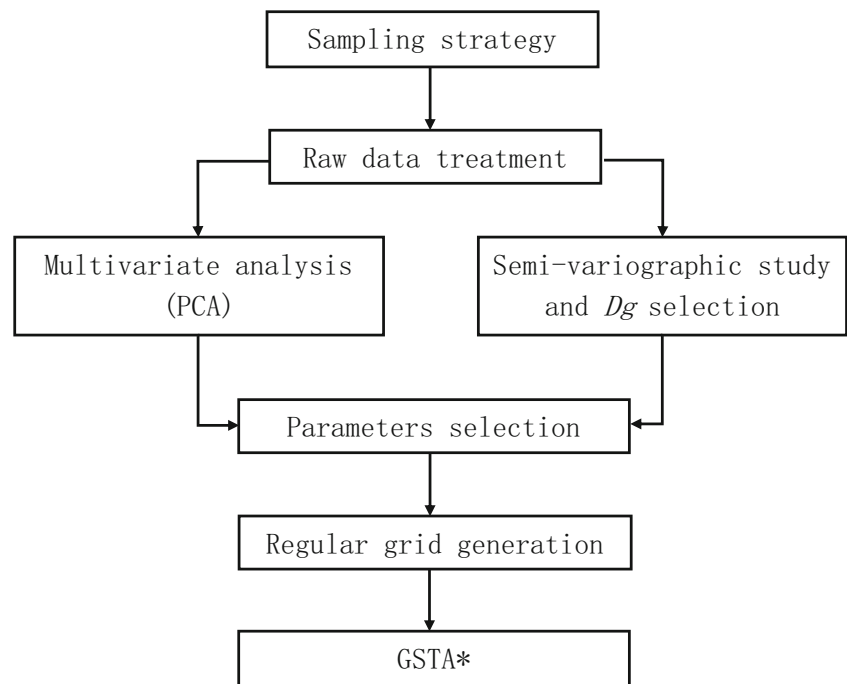
- (1) The southern part of the historical dumping site corresponds to an area prone to erosion due to a high energy level giving rise to the domination of coarse sediment. The high level of agitation is due to the proximity between the historical dumping site dome and the coast [1]. In this area, widely varying TOC and Ca concentrations were observed and the presence of “hot spots” with a high Si concentration directs the vectors.
- (2) At the NE part of the study site, a reverse trend is observed with local “hot spots” with a high TOC and Ca concentration and low Si content increases. These vectors are mainly directed according to the sporadic high concentrations of TOC and Ca. The interpretation of this set of orange vectors may be comparable to that the red vectors (case HHL). Furthermore, some sporadic high values can also be result to vectors direction anomalies.

With the developed GSTA* approach, operated with the three geochemical parameters, the sedimentary processes and the different areas previously defined by Baux et al. [1] have been correctly highlighted with a supply of short-scale information. Ca was excluded from the PCA analysis because the multiple sources of carbonates (whether fine carbonate of continental origin or from marine biogenic sands) confused the message. The GSTA* approach has allowed the geochemical parameters comparison in a spatial way and discriminants the dynamical behaviour of the two types of particles. Moreover, the understanding of the dynamics of fine sediments obtained based on the TOC variability alone, can be enhanced by the combined approach using the three chemical parameters: for example, by identifying the original source of the sand deposits. It can be assumed that the addition of supplementary chemical parameters may upgrade the understanding of the sediment transport: for example, the inclusion of arsenic, a marker of glauconite which is enriched in the littoral sands.

4.5 Discussion on methodology

The GSTA* workflow is proposed on Fig. 5. Seven distinct steps are identified: (1) sampling strategy; (2) raw data treatment; (3) multivariate analysis (PCA); (4) semi-variographic

Fig. 5 The GSTA* workflow



study and Dg determination; (5) parameters selection; (6) regular grid generation and (7) the GSTA*.

Step 1: Sampling strategy

The appropriate sampling strategy will need to be adapted to the scientific objectives and can be very different depending on the study site. To be reliable, the semi-variographic study requires a minimum number of samples. For example, this study is based on 179 samples. Moreover, another important factor to consider is the density of samples across the study area which need to be balanced between (1) a minimum value enough to get sufficient detailed information on the processes of interest and (2) a maximum value to prevent noise sampling. Each sampling scale corresponds to an interpretation scale.

Step 2: Raw data treatment

Geochemical data were previously standardized to set the average of the distribution to 0 and the standard deviation equal to 1. This approach enables the comparison between parameters with very different ranges of values.

Multivariate analysis (PCA) and Semi-variogram study were conducted simultaneously to enable the selection of the most reliable and informative parameters.

Step 3: Multivariate analysis (PCA)

The PCA methodology allows (1) the identification of the different groups of correlated parameters, (2) a progressive

reduction of the number of geochemical parameters and (3) the selection of the best markers for distinguishing samples from each other.

Step 4: Semi-variogram study and Dg determination

This procedure defines the geostatistical distance (Dg) and gives the degree of confidence in a shorter distance (Dg is defined according to the shape of the semi-variogram model). Dg is the optimal distance around a point to establish a vectors. If Dg is too small, there is a loss of relevant information; if Dg is too great, the signal is excessively smoothed. The semi-variogram of chemical data reveals a best spatial dependency (i.e.; the null nugget effect) in comparison with the granulometric data (i.e.; the nugget effect is observed), most probably due to the problem related to the plurimodal data distributions.

Step 5: Parameters selection

The selection of parameters is based on previous multivariate and semi-variogram analyses (quality of data) and will depend on the objective of the study (requiring an expert's opinion).

Step 6: Regular grid generation

The generation of field vectors must be performed based on a regular grid to minimize edge effects and to standardize weight between neighbouring locations.

Step 7: The GSTA*

The trend vectors generated by the GSTA* demonstrate the methodology to be non-subjective, informative and useful in improving the interpretation of the dataset acquired. Many applications might be expected. Work with non-normalized geochemical data allows to preserve the grain size sorting impact and to assess the natural sedimentary dynamic processes. On complementary way, the use of normalized data (for example, normalized on aluminium) lead to the identification of sources and spatial anthropogenic disturbances.

In the studied site, the lack of structuration at a shorter distance with granulometric data do not allow the combination between the granulometric and geochemical parameters, but the combination of these two types of dataset could be consider on another sites.

5 Conclusions and perspectives

The developed GSTA* approach (GSTA adapted to a geochemical study) enabled the combination of several geochemistry elements to describe the dynamic processes, sources, sinks, etc., based on a robust statistical analysis.

In the current version, the “GiSedTrend” plugin is only adapted to granulometric parameters and is difficult to adapt for use with geochemical data.

To avoid anomalies in the vector calculations and any related misinterpretation, improvements could be added to the intra-statistical tests which would consider the quantitative aspects and precision of variables. A new program currently being development by the CNAM-Intechmer team will also allow for the integration of numerous geochemical parameters (>3). It offers promising new perspectives for both geochemists and sedimentologists.

Acknowledgments The authors are grateful to research RIN (“Réseaux d’Intérêts Normands”) for their funding of the SELINe project. We wish to thank to the “Grand Port Maritime du Havre” and the crews of the two ships, “Le Marais” and the “Côtes de la Manche”. We thank all the staffs for assistance in technical operations. The authors would like to express their gratitude to Dr. Colin Burton for his detailed correction of the English used in the manuscript. At least, we greatly thank the anonymous reviewer whose comments and suggestions helped to improve and clarify this manuscript.

References

- Baux, N., Murat, A., Faivre, Q., Lesourd, S., Poizot, E., Méar, Y., Basselet, S., Dauvin, J.-C.: Sediment dynamic equilibrium, a key for assessing a coastal anthropogenic disturbance using geochemical tracers: application to the eastern part of the bay of seine. *Cont. Shelf Res.* **175**, 87–98 (2019). <https://doi.org/10.1016/j.csr.2019.02.002>
- Hopke, P.K., Lamb, R.E., Natusch, D.F.S.: Multielemental characterization of urban roadway dust. *Environ. Sci. Technol.* **14**, 164–172 (1980). <https://doi.org/10.1021/es60162a006>
- Vogt, N.B., Brakstad, F., Thrane, K., Nordenson, S., Krane, J., Aamot, E., Kolset, K., Esbensen, K., Steinnes, E.: Polycyclic aromatic hydrocarbons in soil and air: statistical analysis and classification by the SIMCA method. *Environ. Sci. Technol.* **21**, 35–44 (1987). <https://doi.org/10.1021/es00155a003>
- Pearson, K.: On lines and planes of closet fit to systems of points in space. *Lond. Edinb. Dublin Philos. Mag. J. Sci.* **2**, 559–572 (1901)
- Hotelling, H.: Analysis of a complex of statistical variables into principal components. *J. Educ. Psychol.* **24**, 417–441 (1933). <https://doi.org/10.1037/h0071325>
- Syms, C.: Principal components analysis. In: Jørgensen, S.E., Fath, B.D. (eds.) *Encyclopedia of Ecology*, pp. 2940–2949. Academic Press, Oxford (2008). <https://doi.org/10.1016/B978-008045405-4.00538-3>
- Lewis, P.D., Menzies, G.E.: Vibrational spectra, principal components analysis and the horseshoe effect. *Vib. Spectrosc.* **81**, 62–67 (2015). <https://doi.org/10.1016/j.vibspec.2015.10.002>
- Lee, C.S., Li, X., Shi, W., Cheung, S.C., Thornton, I.: Metal contamination in urban, suburban, and country park soils of Hong Kong: a study based on GIS and multivariate statistics. *Sci. Total Environ.* **356**, 45–61 (2006). <https://doi.org/10.1016/j.scitotenv.2005.03.024>
- Davis, H.T., Marjorie Aelion, C., McDermott, S., Lawson, A.B.: Identifying natural and anthropogenic sources of metals in urban and rural soils using GIS-based data, PCA, and spatial interpolation. *Environ. Pollut.* **157**, 2378–2385 (2009). <https://doi.org/10.1016/j.envpol.2009.03.021>
- Henriksson, S., Hagberg, J., Bäckström, M., Persson, I., Lindström, G.: Assessment of PCDD/fs levels in soil at a contaminated sawmill site in Sweden – a GIS and PCA approach to interpret the contamination pattern and distribution. *Environ. Pollut.* **180**, 19–26 (2013). <https://doi.org/10.1016/j.envpol.2013.05.002>
- Borges, R.C., Caldas, V.G., Filho, F.F.L.S., Ferreira, M.M., Lapa, C.M.F.: Use of GIS for the evaluation of heavy metal contamination in the Cunha Canal watershed and west of the Guanabara Bay, Rio de Janeiro. *RJ. Mar. Pollut. Bull.* **89**, 75–84 (2014). <https://doi.org/10.1016/j.marpolbul.2014.10.033>
- Velasco, V., Tubau, I., Vázquez-Suñé, E., Gogu, R., Gaitanaru, D., Alcaraz, M., Serrano-Juan, A., Fernández-García, D., Garrido, T., Fraile, J., Sanchez-Vila, X.: GIS-based hydrogeochemical analysis tools (QUIMET). *Comput. Geosci.* **70**, 164–180 (2014). <https://doi.org/10.1016/j.cageo.2014.04.01313>
- El-Amier, Y.A., Elnaggar, A.A., El-Alfy, M.A.: Evaluation and mapping spatial distribution of bottom sediment heavy metal contamination in Burullus Lake. *Egypt. J. Basic Appl. Sci.* **4**, 55–66 (2017). <https://doi.org/10.1016/j.ejbas.2016.09.005>
- Hou, D., O’Connor, D., Nathanail, P., Tian, L., Ma, Y.: Integrated GIS and multivariate statistical analysis for regional scale assessment of heavy metal soil contamination: a critical review. *Environ. Pollut.* **231**, 1188–1200 (2017). <https://doi.org/10.1016/j.envpol.2017.07.021>
- Bodrud-Doza, M., Bhuiyan, M.A.H., Islam, S.M.D.-U., Rahman, M.S., Haque, M.M., Fatema, K.J., Ahmed, N., Rakib, M.A., Rahman, M.A.: Hydrogeochemical investigation of groundwater in Dhaka City of Bangladesh using GIS and multivariate statistical techniques. *Groundw. Sustain. Dev.* **8**, 226–244 (2019). <https://doi.org/10.1016/j.gsd.2018.11.008>
- Facchinelli, A., Sacchi, E., Mallen, L.: Multivariate statistical and GIS-based approach to identify heavy metal sources in soils. *Environ. Pollut.* **114**, 313–324 (2001). [https://doi.org/10.1016/S0269-7491\(00\)00243-8](https://doi.org/10.1016/S0269-7491(00)00243-8)

17. Romic, M., Romic, D.: Heavy metals distribution in agricultural topsoils in urban area. *Environ. Geol.* **43**, 795–805 (2003). <https://doi.org/10.1007/s00254-002-0694-9>
18. Duman, M., Duman, Ş., Lyons, T.W., Avci, M., İzdar, E., Demirkurt, E.: Geochemistry and sedimentology of shelf and upper slope sediments of the south-Central Black Sea. *Mar. Geol.* **227**, 51–65 (2006). <https://doi.org/10.1016/j.margeo.2005.11.009>
19. Yesilonis, I.D., Pouyat, R.V., Neerchal, N.K.: Spatial distribution of metals in soils in Baltimore, Maryland: role of native parent material, proximity to major roads, housing age and screening guidelines. *Environ. Pollut.* **156**, 723–731 (2008). <https://doi.org/10.1016/j.envpol.2008.06.010>
20. Lu, A., Wang, J., Qin, X., Wang, K., Han, P., Zhang, S.: Multivariate and geostatistical analyses of the spatial distribution and origin of heavy metals in the agricultural soils in Shunyi, Beijing. *China. Sci. Total Environ.* **425**, 66–74 (2012). <https://doi.org/10.1016/j.scitotenv.2012.03.003>
21. Jin, Y., O'Connor, D., Ok, Y.S., Tsang, D.C.W., Liu, A., Hou, D.: Assessment of sources of heavy metals in soil and dust at children's playgrounds in Beijing using GIS and multivariate statistical analysis. *Environ. Int.* **124**, 320–328 (2019). <https://doi.org/10.1016/j.envint.2019.01.024>
22. Li, T., Sun, G., Yang, C., Liang, K., Ma, S., Huang, L., Luo, W.: Source apportionment and source-to-sink transport of major and trace elements in coastal sediments: combining positive matrix factorization and sediment trend analysis. *Sci. Total Environ.* **651**, 344–356 (2019). <https://doi.org/10.1016/j.scitotenv.2018.09.198>
23. Mc Laren, P.: An interpretation of trends in grain size measures. *J. Sediment. Res.* **51**, 611–624 (1981). <https://doi.org/10.1306/212F7CF2-2B24-11D7-8648000102C1865D>
24. Gao, S., Collins, M.B.: A critique of the. *J. Sediment. Res.* **61**, (1991) <https://archives.datapages.com/data/sepm/journals/v59-62/data/061/061001/0143.htm>
25. Poizot, E., Mear, Y., Thomas, M., Garnaud, S.: The application of geostatistics in defining the characteristic distance for grain size trend analysis. *Comput. Geosci.* **32**, 360–370 (2006). <https://doi.org/10.1016/j.cageo.2005.06.023>
26. Poizot, E., Méar, Y.: Using a GIS to enhance grain size trend analysis. *Environ. Model. Softw.* **25**, 513–525 (2010). <https://doi.org/10.1016/j.envsoft.2009.10.002>
27. Pedreros, R., Howa, H.L., Michel, D.: Application of grain size trend analysis for the determination of sediment transport pathways in intertidal areas. *Mar. Geol.* **135**, 35–49 (1996). [https://doi.org/10.1016/S0025-3227\(96\)00042-4](https://doi.org/10.1016/S0025-3227(96)00042-4)
28. Asselman, N.E.M.: Grain-size trends used to assess the effective discharge for floodplain sedimentation, river Waal, the Netherlands. *J. Sediment. Res.* **69**, 51–61 (1999). <https://doi.org/10.2110/jsr.69.51>
29. Mallet, C., Howa, H., Garlan, T., Sottolichio, A., Le Hir, P., Michel, D.: Utilisation of numerical and statistical techniques to describe sedimentary circulation patterns in the mouth of the Gironde estuary. *Comptes Rendus Académie Sci. - Ser. IIA - Earth Planet. Sci.* **331**, 491–497 (2000). [https://doi.org/10.1016/S1251-8050\(00\)01437-3](https://doi.org/10.1016/S1251-8050(00)01437-3)
30. Vanwesenbeeck, V., Lanckneus, J.: Residual sediment transport paths on a tidal sand Bank: a comparison between the modified McLaren model and Bedform analysis. *J. Sediment. Res.* **70**, 470–477 (2000). <https://doi.org/10.1306/2DC40920-0E47-11D7-8643000102C1865D>
31. Friend, P.L., Velegrakis, A.F., Weatherston, P.D., Collins, M.B.: Sediment transport pathways in a dredged ria system, Southwest England. *Estuar. Coast. Shelf Sci.* **67**, 491–502 (2006). <https://doi.org/10.1016/j.ecss.2005.12.005>
32. Kumar, P.S.R., Dwarakish, G.S., Nujuma, N., Gopinath, D.I.: Long term study of sediment dynamics along Mangalore coast. West Coast India Using Sediment Trend Analysis. *Aquat. Procedia.* **4**, 1545–1552 (2015). <https://doi.org/10.1016/j.aqpro.2015.02.200>
33. Yamashita, S., Naruse, H., Nakajo, T.: Reconstruction of sediment-transport pathways on a modern microtidal coast by a new grain-size trend analysis method. *Prog. Earth Planet. Sci.* **5**, 7 (2018). <https://doi.org/10.1186/s40645-018-0166-9>
34. Oliveira, A., Rocha, F., Rodrigues, A., Jouanneau, J., Dias, A., Weber, O., Gomes, C.: Clay minerals from the sedimentary cover from the northwest Iberian shelf. *Prog. Oceanogr.* **52**, 233–247 (2002). [https://doi.org/10.1016/S0079-6611\(02\)00008-3](https://doi.org/10.1016/S0079-6611(02)00008-3)
35. Dubrulle, C., Lesueur, P., Boust, D., Dugué, O., Poupinet, N., Lafite, R.: Source discrimination of fine-grained deposits occurring on marine beaches: the Calvados beaches (eastern bay of the seine, France). *Estuar. Coast. Shelf Sci.* **72**, 138–154 (2007). <https://doi.org/10.1016/j.ecss.2006.10.021>
36. Petrişor, A.-I., Ianoş, I., Jurea, D., Văidianu, M.-N.: Applications of principal component analysis integrated with GIS. *Procedia Environ. Sci.* **14**, 247–256 (2012). <https://doi.org/10.1016/j.proenv.2012.03.024>
37. Jerosch, K.: Geostatistical mapping and spatial variability of surficial sediment types on the Beaufort shelf based on grain size data. *J. Mar. Syst.* **127**, 5–13 (2013). <https://doi.org/10.1016/j.jmarsys.2012.02.013>
38. Avoine, J., Allen, G.P., Nichols, M., Salomon, J.C., Larsonneur, C.: Suspended-sediment transport in the seine estuary, France: effect of man-made modifications on estuary—shelf sedimentology. *Mar. Geol.* **40**, 119–137 (1981)
39. Larsonneur, C., Auffret, J., Avoine, J.: Etudes hydrosédimentaires en Baie de Seine. (1985)
40. Le Hir, P., Ficht, A., Jacinto, R.S., Lesueur, P., Dupont, J.-P., Lafite, R., Brenon, I., Thouvenin, B., Cugier, P.: Fine sediment transport and accumulations at the mouth of the seine estuary (France). *Estuaries.* **24**, 950–963 (2001)
41. Larsonneur, C.: Manche centrale et baie de Seine : géologie du substratum et des dépôts meubles, (1971)
42. Méar, Y., Poizot, E., Murat, A., Lesueur, P., Thomas, M.: Fine-grained sediment spatial distribution on the basis of a geostatistical analysis: example of the eastern bay of the seine (France). *Cont. Shelf Res.* **26**, 2335–2351 (2006). <https://doi.org/10.1016/j.csr.2006.06.009>
43. Lesourd, S., Lesueur, P., Fisson, C., Dauvin, J.-C.: Sediment evolution in the mouth of the seine estuary (France): a long-term monitoring during the last 150years. *Comptes Rendus Geosci.* **348**, 442–450 (2016). <https://doi.org/10.1016/j.crte.2015.08.001>
44. Brylinski, J.-M., Lagadeuc, Y., Gentilhomme, V., Dupont, J.P., Lafite, R., Dupeuble, P.-A., Huault, M.-F., Auger, Y., Puskaric, E., Wartel, M., Cabioch, L.: Le "fleuve côtier" : un phénomène hydrologique important en Manche orientale : Exemple du Pas-de-Calais. *Oceanol. ACTA. SP*, 197–203 (1991)
45. Crevel, L.: La dynamique sédimentaire en Baie de Seine nord-orientale, fluctuations et evolution de la couverture meuble. In: La Baie de Seine. Colloque National du CNRS, 24–26 avril 1985. pp. 193–200 (1985)
46. Méar, Y., Poizot, E., Murat, A., Beryouni, K., Baux, N., Dauvin, J.-C.: Improving the monitoring of a dumping site in a dynamic environment. Example of the Octeville site (Bay of Seine, English Channel). *Mar. Pollut. Bull.* **129**, 425–437 (2018). <https://doi.org/10.1016/j.marpolbul.2017.10.011>
47. Brasselet, S.: Dragages d'entretien du Grand Port Maritime du Havre. Arrêté interpréfectoral du 26/10/2009 : Renouvellement de l'autorisation de dragage et de l'immersion des produits de dragages d'entretien du GPMH. Demande de renouvellement. Grand Port Maritime du Havre (GPMH) - Service Accès et Environnement Maritime (2014)
48. Reynolds, R.C.: Potassium-rubidium ratios and polymorphism in illites and microclines from the clay size fractions of proterozoic

- carbonate rocks. *Geochim. Cosmochim. Acta.* **27**, 1097–1112 (1963). [https://doi.org/10.1016/0016-7037\(63\)90092-9](https://doi.org/10.1016/0016-7037(63)90092-9)
49. Matheron, G.: Les variables régionalisées et leur estimation. Masson Paris Fr. 1–305 (1965)
 50. Renard, D., Bez, N., Desassis, N., Beucher, H., Ors, F., Freulon, X.: RGeostats: Geostatistical Package version 11.1.1. (2020)
 51. Poizot, E., Méar, Y., Biscara, L.: Sediment trend analysis through the variation of granulometric parameters: a review of theories and applications. *Earth-Sci. Rev.* **86**, 15–41 (2008). <https://doi.org/10.1016/j.earscirev.2007.07.004>
 52. Oliver, M.A., Webster, R.: Kriging: a method of interpolation for geographical information systems. *Int. J. Geogr. Inf. Syst.* **4**, 313–332 (1990). <https://doi.org/10.1080/02693799008941549>
 53. McLaren, P., Bowles, D.: The effects of sediment transport on grain-size distributions. *J. Sediment. Res.* **55**, 457–470 (1985). <https://doi.org/10.1306/212F86FC-2B24-11D7-8648000102C1865D>
 54. Gao, S., Collins, M.B.: Net sediment transport patterns inferred from grain-size trends, based upon definition of “transport vectors.” *Sediment. Geol.* **81**, 47–60 (1992). [https://doi.org/10.1016/0037-0738\(92\)90055-V](https://doi.org/10.1016/0037-0738(92)90055-V)
 55. Poizot, E., Méar, Y.: eCSedtrend: a new software to improve sediment trend analysis. *Comput. Geosci.* **34**, 827–837 (2008). <https://doi.org/10.1016/j.cageo.2007.05.022>
 56. Okada, T., Larcombe, P., Mason, C.: Estimating the spatial distribution of dredged material disposed of at sea using particle-size distributions and metal concentrations. *Mar. Pollut. Bull.* **58**, 1164–1177 (2009). <https://doi.org/10.1016/j.marpolbul.2009.03.023>
 57. Paatero, P., Tapper, U., Aalto, P., Kulmala, M.: Matrix factorization methods for analysing diffusion battery data. *J. Aerosol Sci.* **22**, S273–S276 (1991). [https://doi.org/10.1016/S0021-8502\(05\)80089-8](https://doi.org/10.1016/S0021-8502(05)80089-8)
 58. Song, X.-H., Polissar, A.V., Hopke, P.K.: Sources of fine particle composition in the northeastern US. *Atmos. Environ.* **35**, 5277–5286 (2001). [https://doi.org/10.1016/S1352-2310\(01\)00338-7](https://doi.org/10.1016/S1352-2310(01)00338-7)
 59. Polissar, A.V., Hopke, P.K., Harris, J.M.: Source regions for atmospheric aerosol measured at Barrow, Alaska. *Environ. Sci. Technol.* **35**, 4214–4226 (2001). <https://doi.org/10.1021/es0107529>
 60. Song, Y., Xie, S., Zhang, Y., Zeng, L., Salmon, L.G., Zheng, M.: Source apportionment of PM_{2.5} in Beijing using principal component analysis/absolute principal component scores and UNMIX. *Sci. Total Environ.* **372**, 278–286 (2006). <https://doi.org/10.1016/j.scitotenv.2006.08.041>
 61. Khlaifi, A.: Estimation des sources de pollution atmosphérique par modélisation inverse, (2007)
 62. Gao, S., Collins, M.B.: Analysis of grain size trends, for defining sediment transport pathways in marine environments. *J. Coast. Res.* **10**, 70–78 (1994)
 63. Gao, S., Collins, M.B.: The use of grain size trends in marine sediment dynamics: a review. *Chin. J. Oceanol. Limnol.* **19**, 265–271 (2001). <https://doi.org/10.1007/BF02850664>
 64. Le Roux, J.P., Rojas, E.M.: Sediment transport patterns determined from grain size parameters: overview and state of the art. *Sediment. Geol.* **202**, 473–488 (2007). <https://doi.org/10.1016/j.sedgeo.2007.03.014>
 65. McLaren, P., Hill, S.H., Bowles, D.: Deriving transport pathways in a sediment trend analysis (STA). *Sediment. Geol.* **202**, 489–498 (2007). <https://doi.org/10.1016/j.sedgeo.2007.03.011>
 66. Méar, Y., Poizot, E., Murat, A., Beryouni, K., Baux, N., Dauvin, J.-C.: Improving the monitoring of a dumping site in a dynamic environment. Example of the Octeville site (Bay of Seine, English Channel). *Mar. Pollut. Bull.* (2017). <https://doi.org/10.1016/j.marpolbul.2017.10.011>

Publisher's note Springer Nature remains neutral with regard to jurisdictional claims in published maps and institutional affiliations.